Journal of Building Pathology and Rehabilitation (2024) 9:132
https://doi.org/10.1007/s41024-024-00487-3

RESEARCH ARTICLE

Fracture assessment of concrete through digital image correlation (DIC) technique

Sudhanshu S. Pathak[1] · Gaurang R. Vesmawala[2] · Rohini Khandelwal[1] · Aradhana Chavan[1] · Sachin Mane[1] · Sharmistha Chakraborty[1]

Received: 18 July 2024 / Revised: 10 August 2024 / Accepted: 14 August 2024

Abstract
This paper describes the fracture properties of concrete containing Nano TiO_2 (NT) 1%, 2%, 3% and 4% along with fly ash (FA) 30%. The three point bend test was conducted according to size effect method (SEM). The displacement parameters were studied using digital image correlation (DIC). The displacement fields measured using DIC was very well matched with the experimental observations. The results reveal, DIC is helpful to measuring crack opening at different crack locations and the plot of load Vs crack opening displacement shown similar behavior in both methods. For fracture tests, the use of 3% NT with 30% FA is having high fracture energy, while the concrete with 4% NT with 30% FA has low fracture energy. Moreover the use of 4% NT with 30% FA shows the high fracture toughness while the 1% NT with 30% FA shows low fracture toughness.

Keywords Fracture properties · Digital image correlation · Fly ash · Nano TiO_2 · Concrete

1 Theoretical background

Concrete has been used widely and it has been modified according to the requirement such as High performance concrete (HPC), Ultra high performance concrete (UHPC), Self-compacting concrete (SCC), etc. due to its many advantages such as durability, low cost, greater strength etc. [8]. [37] mentioned about the use of SCC is designed for high formwork filling capacity, for good stability etc. [41] mentioned about the usage of cement leads to have adverse impact on environment in terms of emission of CO_2, the cement produces around 7% greenhouse gases. The SCC has been introduced as environmental friendly material, which can be mold into any shape, with improved durability, with remarkable improved fresh properties [30]. The recycled aggregate concrete (RAC) has created interest due to its economic and environmental aspects, the RCA absorbs more water and increases its shrinkage, the use of steel fibers in RCA concrete improves the mechanical properties of concrete [9].

✉ Sudhanshu S. Pathak
pathaksudhanshu2009@gmail.com

[1] Department of Civil Engineering, D Y Patil College of Engineering, Akurdi, Pune, India

[2] Department of Civil Engineering, Sardar Vallabhbhai National Institute of Technology, Surat, Gujarat, India

[20] stated that, the fracture energy will get affected by w/c ratio of the mix, it is decreased with increase in w/c ratio. [5] used w/c ratio in SCC from 0.35 to 0.7, the fracture toughness of w/c ratio 0.7 observed highest and fracture energy observed maximum at w/c ratio 0.4. [6, 7] mentioned about the fracture parameters for SCC and effect of maximum size of aggregate on it and it has been observed that as aggregate size increases the fracture properties of SCC improved significant. [6, 7] investigated the fracture parameters for SCC with volume and size of coarse aggregate, the results are in line with work done by [2, 6, 7, 19, 29] regarding the increase in volume of coarse aggregate leads to increase in fracture energy of concrete. [14] investigated fracture properties of SCC by SEM and work of fracture method (WFM) on notched beams. The WFM shows the correlation of compressive strength and fracture energy, the fracture energy increases with increase in compressive strength while in SEM fracture energy slightly decreases with increase in compressive strength. [23] stated that the due to higher w/c the concrete is identified as a brittle material when tested under three point bend test and concluded that three point bend test and wedge splitting test (WPT) are influenced by strength of cement paste and amount of coarse aggregate used respectively.

[38] mentioned the mechanical and fracture parameters are strongly affected by amount fibers used and type of fiber

Published online: 23 August 2024

Table 1 Mix proportions

Specimen ids	Cement (kg/m^3)	w/c	Fly ash (kg/m^3)	TiO_2 (kg/m^3)	Fine aggregate (kg/m^3)	Coarse aggregate (kg/m^3)	Superplasticizer (% of cement)
CC	430	0.38	–	–	640	1142	0.6
NT1FA30	296.7	0.38	129	4.3	640	1142	0.6
NT2FA30	292.4	0.38	129	8.6	640	1142	0.6
NT3FA30	288.1	0.38	129	12.9	640	1142	0.6
NT4FA30	283.8	0.38	129	17.2	640	1142	0.6

used in concrete, same is the case observed by [1, 4, 13, 16, 24, 28] and [22]. [31, 36] has used fly ash based geo polymer concrete (GPC) for study and concluded that fracture energy observed with GPC found similar to Ordinary Portland cement (OPC), the compressive strength is directly proportional to fracture energy. [21, 27] observed, generally Nano material are having issue related to dispersion in concrete, many Nano material required ultra-sonication treatment for effective dispersion of particles. TiO_2 particles are adhering to self-assembled monolayer due to which the ultra-sonication can be eliminated and effective dispersion of particles can takes place easily.

DIC technique has increasing the attention of researchers as it provides the information about the crack opening displacement (COD) [42]. [10, 12] used DIC for mortar in which the OPC is partially replaced with limestone/metakaoline, the results obtained through DIC are very well matching with results obtained through experiment. [43] and [11, 25] used DIC and acoustic emission (AE) technique for examination of fracture in concrete and concluded that the AE technique is suitable to identification of fracture growth which was happened due to macro crack and DIC will useful for opening of cracks at various locations. [40] used DIC in concrete using multi wall carbon Nano tubes (MWCNT), Nano silica, Nano alumina etc. and concluded that DIC technique is effective while conducting fracture test for determination of crack length. [35] mentioned that, the use of higher amount of FA used in concrete leads to have many voids in concrete and they will be different from dense structure. [26] served the water to binder ratio has a significant effect, the concrete with low water to binder ratio the peak load increases and increase in volume of fibers also increases the peak load.

2 Preparation of specimens and experimental setup

The three point bend test (TPB) was performed confirming to [32]. The concrete beams were prepared according to mix design shown in Table 1. Nano TiO_2 was used along with F class fly ash. Ordinary Portland cement (OPC) 53 grade was used for the all mixes confirming to IS 12269-2013 (IS 12269-2013). For dispersion of Nano TiO_2 particles, polycarboxylate based superplasticizer was used. [15, 41] reported the use of polycarboxylate based superplasticizer showed great effect on dispersion properties of Nano particles. Also ultra-sonication was adopted to avoid the accumulation of Nano particles. The coarse aggregate was used with fineness modulus of 2.65, a specific gravity of 2.85 and water absorption 1.4%. The maximum size of coarse aggregate (d_a) is 20 mm having specific gravity 2.7 and absorption of water 0.85%. The 1, 2, 3 and 4% of NT used along with constant 30 percentage of FA with constant w/c ratio 0.38.

To evaluate the fracture properties of concrete, the geometrical similar beams of size $74.90 \times 74.90 \times 200$ mm, $74.90 \times 149.80 \times 400$ mm, $74.90 \times 299.60 \times 600$ mm (Width × Depth × Length) (Figs. 1, 2) were prepared by Size effect method (SEM) confirming to [33] recommendations. The length to depth (*l*/*d*) ratio was kept 2.67 and notch is provided at center of beam with the beam depth ratio of 0.25. A 2 mm thick notch having 25 mm depth was prepared while casting the specimens; the steel plate was inserted in the mold and the same has been removed after 24 h. The demolded specimens were kept for curing in curing tank till the date of testing. A closed loop servo control machine with the capacity of 50kN (Fig. 3) with CMOD opening of 0.03 mm/min. In addition to that the $150 \times 150 \times 700$ mm beams, $150 \times 150 \times 150$ mm cubes and 150 mm diameter and 300 mm height cylinder were casted with reference to ASTM C 78 (ASTM Standard C78), IS 516-1959 (IS 516-1959) and ASTM C 469 [3] to understand the flexure, compressive and split tensile strength of concrete respectively.

3 Digital image correlation technique and evaluation of opening displacement

DIC useful for measurement of displacement of spackles in a digital image. Which is noncontact measurement technique which helps to get the data related displacement of the surface of specimen. The specimens were painted by black and white paint to improve the correlation of image. The images were captured before and after at various stages of loading and unloading with the help of digital camera. The images were captured at rate of 5 s per

Fig. 1 Beam specimens

Fig. 2 Molds of specimens for concrete

Fig. 3 Experimental set up for fracture test

image at far distance from testing setup using remote to avoid the vibrations and disturbance. The distance between camera lens and specimen kept constant throughout the experiment as shown in Fig. 4. The intensity and positions of lights are kept constant throughout the experiment. In DIC technique, the correlation between the deformed and undeformed images is measured to study the displacement fields. A point in (x, y) in the undeformed (original) image is correlated with a point (x^*, y^*) in the deformed image as mentioned in Eq. 1 and Fig. 5. A suitable region of interest is chosen as shown in Fig. 6 and with help of VIC 2D software displacement fields are measured.

$$x^* = x + \mu(x, y)$$

$$y^* = y + v(x, y) \quad (1)$$

The μ and v represents horizontal and vertical displacement respectively, these displacement fields are measured by

Fig. 4 Experimental setup for DIC

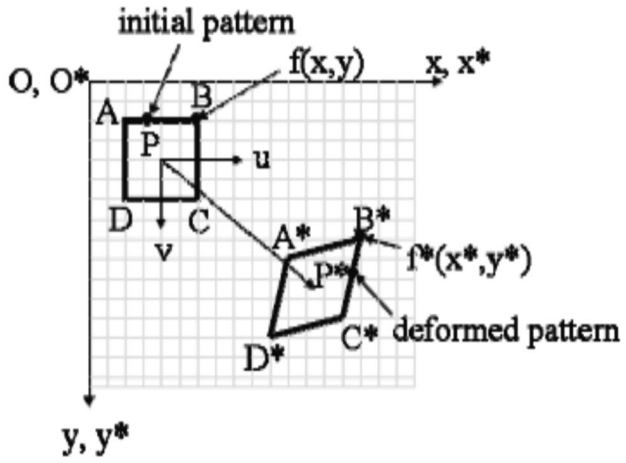

Fig. 5 Deformed and undeform pattern of image

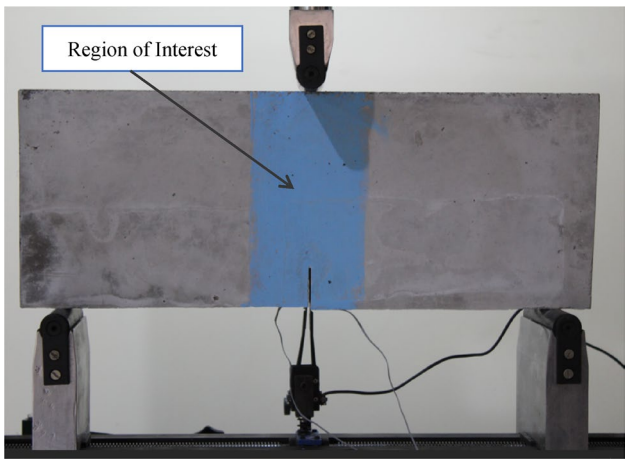

Fig. 6 Region of interest for DIC study

minimization of the correlation coefficient (C), which can be states as,

$$C = \frac{\sum[G(x,y) - H(x^*y^*)]^2}{\sum[G^2(x,y)]} \quad (2)$$

where, G and H are grey scale light intensity with respect to point, the crack opening displacement and the crack extension can be determined from the u-displacement field findings.

4 Results and discussion

4.1 Mechanical and fracture properties

Table 2 and Figs. 7, 8 shows the detailed results of compressive strength, flexure strength, split tensile strength and fracture energy. The compressive strength of control concrete (CC) was observed 52.21 N/mm^2, the NT3FA30 observed high compressive strength (56.02 N/mm^2) compared with all the mixes and NT1FA30 found low (50.20 N/mm^2) in all the mixes. Which indicates compressive strength increases from 1% NT to 3% NT and declines after 3% NT. The same is the case for flexural strength and split tensile strength, the NT3FA30 found high 8.87 N/mm^2 and 4.25 N/mm^2 respectively which indicates the 3% NT observed to be an optimum dose for as far as mechanical properties of concrete. Figure 8 shows the fracture energy details, which clearly states that the fracture energy increases with increase in NT 1% to 3% and after 3% it declines, which may happen due to leaching out of excess amount of Nano particles as observed by [18]. The NT3FA30 observed highest fracture energy which is improved about 10.93% compared with CC. Regarding fracture toughness, it has been observed that the fracture toughness increases with increase in NT percent from 1 to 4 and 4%, which is improved around 31.49% compared with CC. As per [17] the most favorable fracture toughness was observed at 20% of FA. The [39] observed the use of FA showed better performance in fracture and mechanical properties of concrete. The NT gives better results in fracture and mechanical properties this will have great impact of dispersion of Nano particles mentioned by [34], the has been observed in present study.

The plot of Load Vs CMOD graphs is shown in Fig. 9. NT4FA30 mix shows the highest peak load and lower that CC, which indicates the use of FA and NT as replacement to OPC improves the peak load conditions.

4.2 Digital image correlation

The load vs crack opening displacement responses are shown in Fig. 10, on the curve P1–P4 points represents the

Table 2 Details of mechanical and fracture properties

Specimen ids	f_c (MPa)	f_t (MPa)	f_r (MPa)	G_F (N/m)	K_{Ic} (MPa $m^{0.5}$)
CC	52.21	2.35	5.45	77.44	0.87
NT1FA30	50.20	2.55	6.09	79.13	0.69
NT2FA30	53.52	3.05	7.35	80.11	0.82
NT3FA30	56.02	4.25	8.87	86.95	0.92
NT4FA30	52.50	4.15	7.90	77.36	1.27

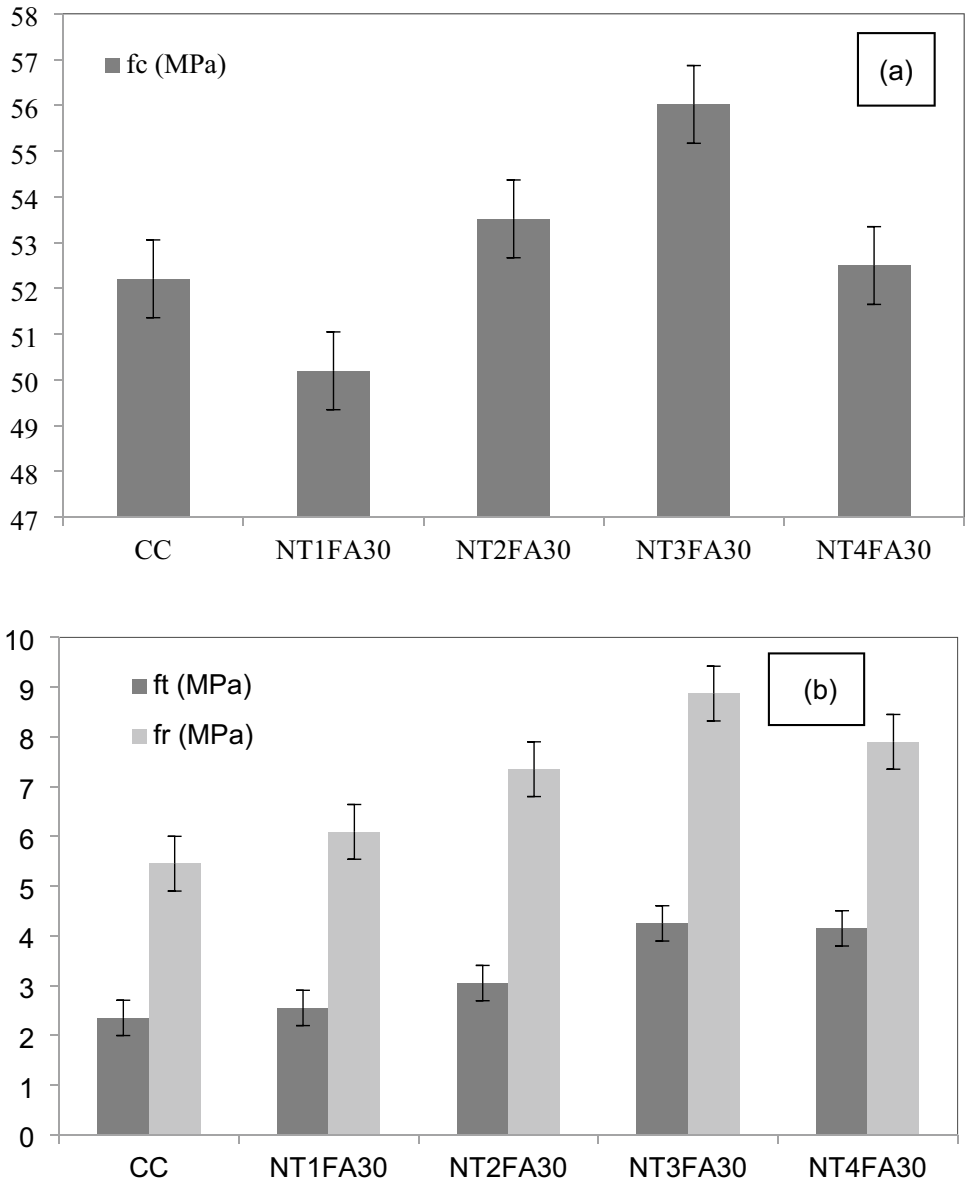

Fig. 7 Results **a** Compressive strength, **b** Tensile strength and flexural strength

displacement at different stages, the changes happening in crack extension can be observed. The first image represents pre-cracking phase.

Displacement of concrete beams are shown in Fig. 11, the first point P1 represents point at before cracking. The crack extension and crack opening is zero which indicates the uniform horizontal displacement near notch. Second point P2 represents point represents crack propagation the crack is visible at this stage which is stable. Third point P3 represents extension of crack which is in unstable. Fourth image P4 represents unstable extension of crack at crack tip of the specimen. The sharp transformation of crack extension is observed from P2 to P3 and P3 to P4 and that is clearly visible. The vertical displacement at notch point of specimen is measured by using LVDT and DIC (Fig. 12). It has been seen very good relation has been observed between displacement measured using DIC techniques and by using LVDT. Which indicated the effective usefulness of DIC technique.

5 Conclusion

The conclusion made from the work is as follows:

1. The results obtained from experiment shows that, the 3% NT has a great influence on fracture energy which is improved by 10.93% compared with control concrete.

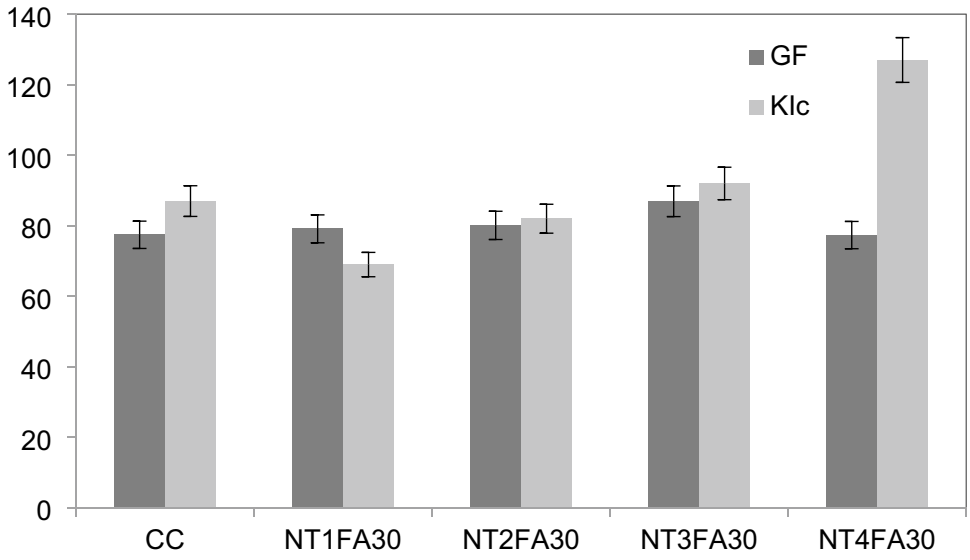

Fig. 8 Results of fracture energy and fracture toughness

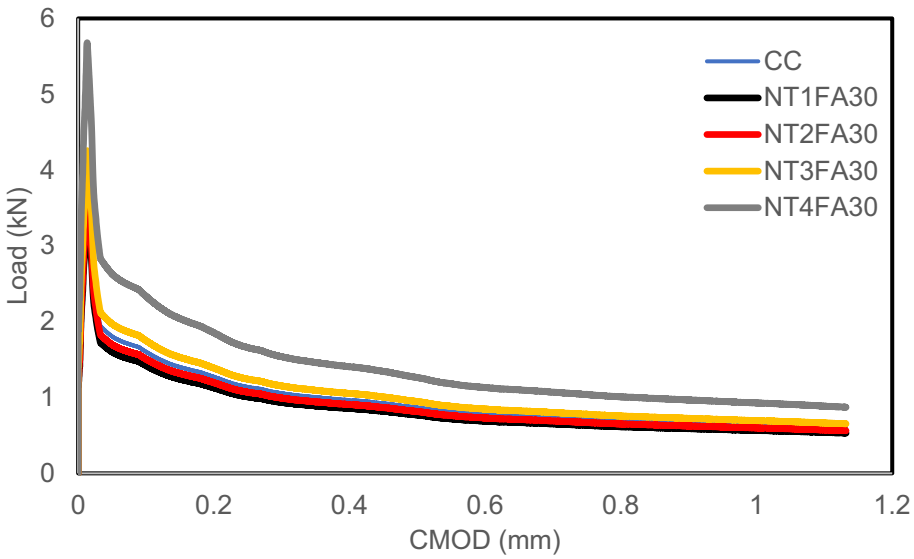

Fig. 9 Plot of load vs CMOD

2. The fracture energy increased from 1 to 3% NT and after 3% NT it declines, which indicate the excess amount of NT may have adverse impact on fracture energy.
3. The compressive strength, split tensile strength and flexural strength increases from 1 to 3% NT and after 3% NT it declines.
4. The fracture toughness increases with increase in NT from 1 to 4% and NT 4% has shown high fracture toughness, which is significantly improved by 31.49% compared with control concrete.
5. The peak load is increased with increase in size of specimen in all mixes.
6. DIC is an efficient approach for measuring fracture lengths and crack opening.
7. A good acceptable relation is observed in crack opening displacement and displacement measured by DIC and using clip gauge.
8. It can be summarizes that, the substitute for traditional way of measurement by using clip gauges and LVDTs is simple DIC technique can be very much useful.

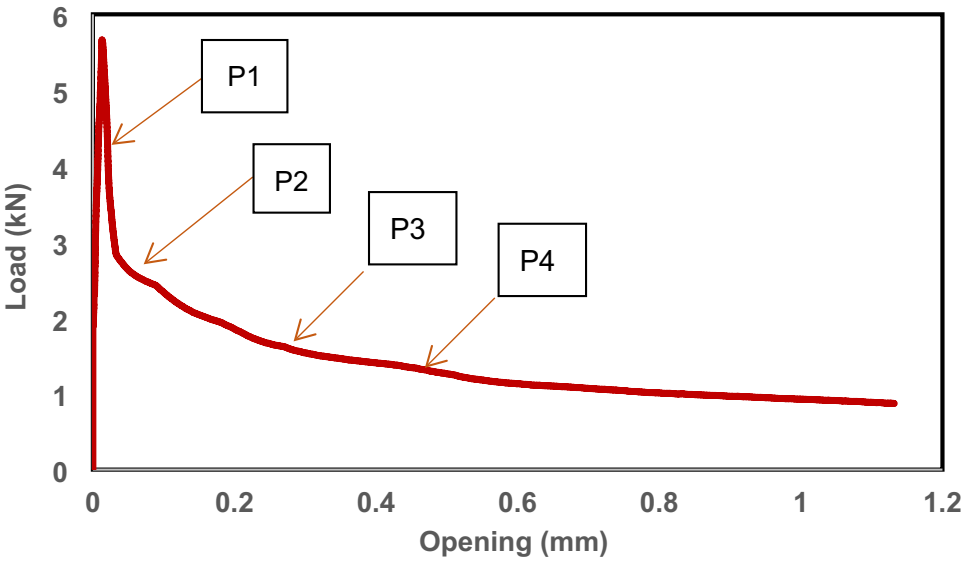

Fig. 10 Load vs CMOD of notched beam specimen

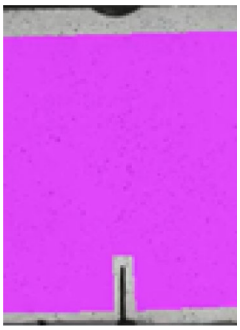

P1 (Point before cracking)
CMOD 0.0038 mm
Load <0.5 Load $_{Max}$
CTOD 0 mm

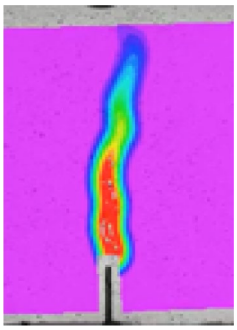

P2 (Point during crack propagation)
CMOD 0.58 mm
Load = 0.95 Load $_{Max}$
CTOD 0.010 mm

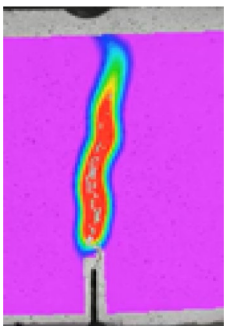

P3 (Point of extension of crack)
CMOD 0.90 mm
Load = 0.75 Load $_{Max}$
CTOD 0.107 mm

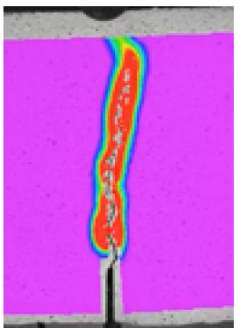

P4 (Point of unstable extension of crack)
CMOD 1.12 mm
Load = 0.95 Load $_{Max}$
CTOD 0.114 mm

Fig. 11 Horizontal displacements at various stages of loading

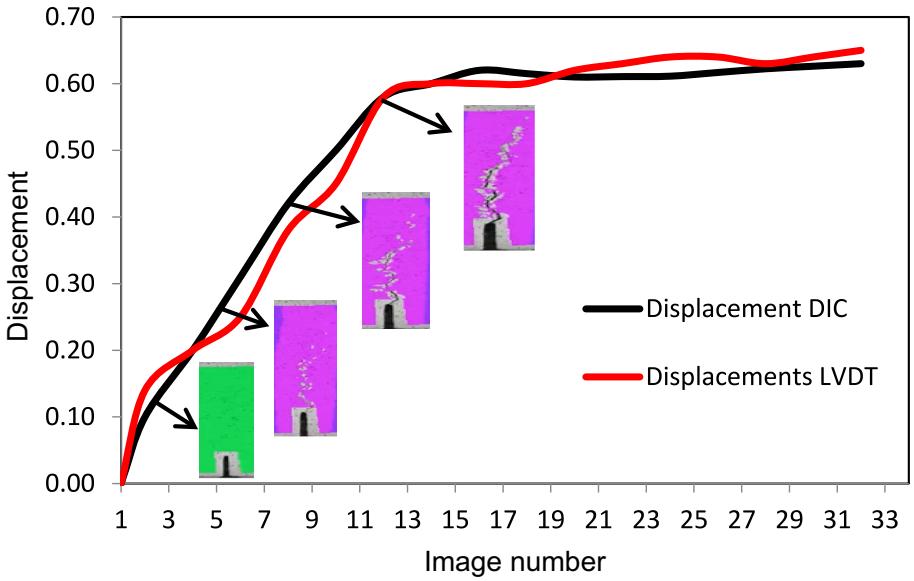

Fig. 12 Displacement vs Image number

Author contributions Sudhanshu Pathak, Sharmistha Chakraborty and Aradhana Chavan Prepared manuscript Sachin Mane, Rohini Khandelwal Reviewed manuscript Gaurang Vesmawala: Conceptualization, Equipment and other resources arrangements.

Funding The authors declare that no funds, grants, or other support were received during the preparation of this manuscript.

Data availability No datasets were generated or analysed during the current study.

Declarations

Conflict of interest The author declares that they have no known competing financial interests that could have appeared to influence the work reported in this paper. Also, the authors declare that there is no conflict of interest regarding the publication of this paper.

References

1. Alberti MG, Enfedaque A, Gálvez JC (2014) On the mechanical properties and fracture behavior of polyolefin fiber-reinforced self-compacting concrete. Constr Build Mater 55:274–288. https://doi.org/10.1016/j.conbuildmat.2014.01.024
2. Alyhya WS, Abo Dhaheer MS, Al-Rubaye MM, Karihaloo BL (2016) Influence of mix composition and strength on the fracture properties of self-compacting concrete. Constr Build Mater 110:312–322. https://doi.org/10.1016/j.conbuildmat.2016.02.037
3. ASTM Standard C469, C469M (2014) Standard test method for static modulus of elasticity and poisson's ratio of concrete in compression. ASTM International. https://doi.org/10.1520/C0469
4. Bencardino F, Rizzuti L, Spadea G, Swamy RN (2010) Composites: part B experimental evaluation of fiber reinforced concrete fracture properties. Compos Part B: Eng 41(1):17–24. https://doi.org/10.1016/j.compositesb.2009.09.002
5. Beygi MHA, Kazemi MT, Nikbin IM, Amiri JV (2013) The effect of water to cement ratio on fracture parameters and brittleness of self-compacting concrete. Mater Des 50:267–276. https://doi.org/10.1016/j.matdes.2013.02.018
6. Beygi MHA, Kazemi MT, Nikbin IM, Vaseghi Amiri J, Rabbanifar S, Rahmani E (2014) The influence of coarse aggregate size and volume on the fracture behavior and brittleness of self-compacting concrete. Cem Concr Res 66:75–90. https://doi.org/10.1016/j.cemconres.2014.06.008
7. Beygi MHA, Kazemi MT, Vaseghi Amiri J, Nikbin IM, Rabbanifar S, Rahmani E (2014) Evaluation of the effect of maximum aggregate size on fracture behavior of self compacting concrete. Constr Build Mater 55:202–211. https://doi.org/10.1016/j.conbuildmat.2014.01.065
8. Cheah CB, Tiong LL, Ng EP, Oo CW (2019) The engineering performance of concrete containing high volume of ground granulated blast furnace slag and pulverized fly ash with polycarboxylate-based superplasticizer. Constr Build Mater 202:909–921. https://doi.org/10.1016/j.conbuildmat.2019.01.075
9. Chen GM, Yang H, Lin CJ, Chen JF, He YH, Zhang HZ (2016) Fracture behaviour of steel fibre reinforced recycled aggregate concrete after exposure to elevated temperatures. Constr Build Mater 128:272–286. https://doi.org/10.1016/j.conbuildmat.2016.10.072
10. Das S, Aguayo M, Dey V, Kachala R, Mobasher B, Sant G, Neithalath N (2014) Cement and concrete composites the fracture response of blended formulations containing limestone powder: evaluations using two-parameter fracture model and digital image correlation. Cement Concrete Composites 53:316–326. https://doi.org/10.1016/j.cemconcomp.2014.07.018
11. Dong M, Elchalakani M, Karrech A, Pham TM, Yang B (2019) Glass fibre-reinforced polymer circular alkali-activated fly ash/slag concrete members under combined loading. Eng Struct 199:109598. https://doi.org/10.1016/j.engstruct.2019.109598
12. Dong W, Rong H, Wu Q, Li J (2018) Investigations on the FPZ evolution of concrete after sustained loading by means of the DIC technique. Constr Build Mater 188:49–57. https://doi.org/10.1016/j.conbuildmat.2018.08.077
13. Elices M, Guinea GV, Planas J (1997) On the measurement of concrete fracture energy using three-point bend tests. Mater Struct 30(6):375–376. https://doi.org/10.1007/BF02480689

14. Eskandari H, Muralidhara S, Raghu Prasad BK, Venkatarama Reddy BV (2010) Size effect in self consolidating concrete beams with and without notches. Sadhana-Acad Proceed Eng Sci 35(3):303–317. https://doi.org/10.1007/s12046-010-0012-2
15. Feng P, Chang H, Liu X, Ye S, Shu X, Ran Q (2020) The significance of dispersion of nano-SiO2 on early age hydration of cement pastes. Mater Des 186:108320. https://doi.org/10.1016/j.matdes.2019.108320
16. Gesoglu M (2015) Fracture behavior and mechanical properties of concrete with artificial lightweight aggregate and steel fiber. Constr Build Mater 84:156–168. https://doi.org/10.1016/j.conbuildmat.2015.03.054
17. Gil DM,Golewski GL (2018) Effect of silica fume and siliceous fly ash addition on the fracture toughness of plain concrete in mode i. IOP conference series: materials science and engineering. 416 (1). https://doi.org/10.1088/1757-899X/416/1/012065
18. Jalal M, Fathi M, Farzad M (2013) Effects of fly ash and TiO2nanoparticles on rheological, mechanical, microstructural and thermal properties of high strength self compacting concrete. Mech Mater 61:11–27. https://doi.org/10.1016/j.mechmat.2013.01.010
19. Karamloo M, Mazloom M, Payganeh G (2016) Effects of maximum aggregate size on fracture behaviors of self-compacting lightweight concrete. Constr Build Mater 123:508–515. https://doi.org/10.1016/j.conbuildmat.2016.07.061
20. Karamloo M, Mazloom M, Payganeh G (2016) Influences of water to cement ratio on brittleness and fracture parameters of self-compacting lightweight concrete. Eng Fract Mech 168:227–241. https://doi.org/10.1016/j.engfracmech.2016.09.011
21. Khataee R, Heydari V, Moradkhannejhad L, Safarpour M, Joo SW (2013) Self-cleaning and mechanical properties of modified white cement with nanostructured TiO_2. J Nanosci Nanotechnol 13(7):5109–5114. https://doi.org/10.1166/jnn.2013.7586
22. Kizilkanat AB, Kabay N, Akyüncü V, Chowdhury S, Akça AH (2015) Mechanical properties and fracture behavior of basalt and glass fiber reinforced concrete: an experimental study. Constr Build Mater 100:218–224. https://doi.org/10.1016/j.conbuildmat.2015.10.006
23. Korte S, Boel V, De Corte W, De Schutter G (2014) Static and fatigue fracture mechanics properties of self-compacting concrete using three-point bending tests and wedge-splitting tests. Constr Build Mater 57:1–8. https://doi.org/10.1016/j.conbuildmat.2014.01.090
24. Kosior-kazberuk M, Berkowski P (2016) Fracture mechanics parameters of fine grained concrete with polypropylene fibres. Procedia Eng 161:157–162. https://doi.org/10.1016/j.proeng.2016.08.515
25. Li S, Fan X, Chen X, Liu S, Guo Y (2020) Development of fracture process zone in full-graded dam concrete under three-point bending by DIC and acoustic emission. Eng Fract Mech 230:106972. https://doi.org/10.1016/j.engfracmech.2020.106972
26. Löfgren I, Stang H, Olesen JF (2005) Fracture properties of FRC determined through inverse analysis of wedge splitting and three-point bending tests. J Adv Concr Technol 3(3):423–434. https://doi.org/10.3151/jact.3.423
27. Masuda Y, Saito N, Hoffmann R, De Guire MR, Koumoto K (2003) Nano/micro-patterning of anatase TiO2 thin film from an aqueous solution by site-selective elimination method. Sci Technol Adv Mater 4(5):461–467. https://doi.org/10.1016/j.stam.2003.08.002
28. Najim KB, Saeb A, Al-azzawi Z (2018) Author 's accepted manuscript. J Build Eng. https://doi.org/10.1016/j.jobe.2018.02.014
29. Nikbin IM, Beygi MHA, Kazemi MT, Vaseghi Amiri J, Rahmani E, Rabbanifar S, Eslami M (2014) Effect of coarse aggregate volume on fracture behavior of self compacting concrete. Constr Build Mater 52:137–145. https://doi.org/10.1016/j.conbuildmat.2013.11.041
30. Nikbin IM, Davoodi MR, Fallahnejad H, Rahimi S, Farahbod F (2016) Influence of mineral powder content on the fracture behaviors and ductility of self-compacting concrete. J Mater Civil Eng 28(3):1–14. https://doi.org/10.1061/(ASCE)MT.1943-5533.0001404
31. Pfeiffer PA (1988) Determination of fracture energy from size effect and brittleness number. ACI Mater J 84(6):463–480
32. RILEM (1985) Determination of the fracture energy of mortar and concrete by means of three-point bend tests on notched beams (Draft recommendation FMC 50). Mater Struct 18(6):484
33. RILEM (1991) Fracture mechanics of concrete: test methods: size-effect method for determining fracture energy and process zone size of concrete (Draft recommendation TC 89-FMT). Mater Struct 23:461–465
34. Roberto S, Dantas A, Serafini R, Cesar R, Romano DO, Vittorino F, Loh K (2019) Influence of the nano TiO 2 dispersion procedure on fresh and hardened rendering mortar properties. Constr Build Mater. 215:544–556. https://doi.org/10.1016/j.conbuildmat.2019.04.190
35. Rooholamini H, Bayat A, Kazemian F (2022) Mechanical and fracture properties of alkali activated concrete containing different pozzolanic materials. Road Mater Pavement Des 23(4):802–821. https://doi.org/10.1080/14680629.2020.1845783
36. Sarker PK, Haque R, Ramgolam KV (2013) Fracture properties of geopolymer concrete cured in ambient temperature. J Mater Des 44:580–586. https://doi.org/10.1016/j.matdes.2012.08.005
37. Shah SG, Patel BG, Desai AK (2016) Fracture and size effect studies on fibre reinforced self compacting concrete using digital image correlation. 9th International Conference on Fracture mechanics of concrete nd concrete structures (Fram-Cos9). https://doi.org/10.21012/FC9.096
38. Sucharda O, Pajak M, Ponikiewski T, Konecny P (2017) Identification of mechanical and fracture properties of self-compacting concrete beams with different types of steel fibres using inverse analysis. Constr Build Mater 138:263–275. https://doi.org/10.1016/j.conbuildmat.2017.01.077
39. Tang WC, Lo TY (2009) Mechanical and fracture properties of normal-and high-strength concretes with fly ash after exposure to high temperatures. Mag Concr Res 61(5):323–330. https://doi.org/10.1680/macr.2008.00084
40. Vaghela A, Vesmawala G (2022) DIC analysis of nano concrete using functionalized and dispersed carbon nanotubes. Mater Today: Proceed 57:812–817. https://doi.org/10.1016/j.matpr.2022.02.405
41. Vesmawala GR, Vaghela AR, Yadav KD, Patil Y (2019) Effectiveness of polycarboxylate as a dispersant of carbon nanotubes in concrete. Mater Today: Proceed 28:1170–1174. https://doi.org/10.1016/j.matpr.2020.01.102
42. Wang Y, Hu S, He Z (2021) Mechanical and fracture properties of geopolymer concrete with basalt fiber using digital image correlation. Theoret Appl Fract Mech 112:102909. https://doi.org/10.1016/j.tafmec.2021.102909
43. Yasir S, Saliba J, Loukili A (2014) Fracture examination in concrete through combined digital image correlation and acoustic emission techniques. Constr Build Mater 69:232–242. https://doi.org/10.1016/j.conbuildmat.2014.07.044